Data Repository Item 2006062

Sample Details

The sample was collected from core recovered during Ocean Drilling Program (ODP) Leg 176 from Hole 735B, located 93 km south of the ultra-slow spreading Southwest Indian Ridge (32º43.392'S, 57º15.960'E) in a mean water depth of 735m (Fig. 1). This core consists predominantly of gabbro or olivine gabbro, but comprises a series of different litho-stratigraphic units (Units I-XII) and represents the most complete in-situ section of lower ocean crust ever examined (Dick et al., 2000). Results from leg 176 show that zones of deformation in slow-spreading oceanic crust record a complex deformation history, with different units displaying heterogeneous deformation characterized by syn-magmatic and sub-solidus crystal-plastic deformation at granulite to amphibolite facies conditions through to brittle fracture and cataclasis, often associated with hydrothermal activity (Dick et al., 2000; Bach et al., 2001; Natland and Dick, 2001).

The sample, 176-735B-162R-6-22-24, is olivine gabbro that comes from the lower part of hole 735B, 1089m below the sea floor and was collected from unit XI. The sample contains three distinct zones. In zone 1, there has been extensive deformation resulting in alternating bands of partially-recrystallized clinopyroxene and fully recrystallized plagioclase. The clinopyroxene is found as large porphyroclasts with recrystallized tails that form long ribbons. Several such ribbons have been partly altered to amphibole at their edges. Within this zone, concentration of ilmenite and magnetite indicate the intrusion of late-stage melts into the deforming host associated with amphibolite-facies deformation (Trimby, 2005). In zone 2, there are many individual grains of plagioclase and clinopyroxene in a matrix of Fe-Ti oxides. The boundary with zone 1 is sharp, and there are no ribbons or bands of individual phases. Fe-Ti-oxides constitute ~50% of this zone. Zone 3 is essentially undeformed. Large grains of plagioclase and clinopyroxene show limited strain features (e.g. undulose extinction and deformation twins), whilst the oxides are coarse grained ($d > 200$ μm) and form selvages between the other phases. The zircon studied here comes from zone 1.

Methodologies

A petrographic thin section of the sample, polished with progressively finer grades of diamond paste (down to 0.25μm), was given a final polish for 4.5 hours using a colloidal silica (0.06μm) suspension on a polyurethane lap mounted on a Beuhler VibrometII polisher to remove all remaining surface damage. Electron backscatter diffraction (EBSD) data were collected at the Microstructural Analysis Facility housed at Curtin University of Technology and part of the Western Australia Centre for Microscopy, and at HKL Technology, Denmark. The Curtin EBSD system is housed on a Phillips XL30 scanning electron microscope (SEM) and uses a Nordlys I EBSD detector to collect electron backscatter patterns (EBSPs). Orientation contrast images (Fig. 1) were collected from two forescatter detectors that are integrated into the Nordlys detector. Data collected at HKL Technology were obtained on a variable pressure, LEO FEG-SEM. For EBSD analyses and orientation contrast imaging, scanning electron microscope (SEM) operating conditions were 20kV and spot size *c.*0.5μm and the thin section was tilted to 70°.

For this study, a single zircon grain was analyzed by automatically collecting electron backscatter patterns (EBSPs) from a user-defined grid using HKL Technology's Channel 5 Flamenco software. Two orientation maps were made. The first collected orientation data from the whole of the zircon grain (area = 0.35mm^2) using a spaced 3μm grid (Fig. 2a). The second map was a more detailed analysis of a deformed tip of the grain (area B = 0.12mm^2) with EBSPs collected using a 1μm grid (Fig. 2c). At each grid node the collected EBSP was automatically indexed by comparison with theoretical zircon diffraction patterns by HKL Channel 5 Flamenco software. The closeness of fit between observed and theoretical diffraction patterns was high (average "mean angular deviation" of 0.57). Indexing in this way provides crystallographic orientation data at each grid node location. EBSD maps were then produced (using HKL Channel 5 Tango software) by plotting the orientation data for each grid node using the "texture component" feature. Data presented in the maps was noise reduced using the Channel 5 "wildspike" correction to remove isolated erroneously indexed points, and by a four-neighbor zero solution extrapolation to fill some non-indexed points. The orientation data from an analysis at the

grain centre indicate that the zircon has been cut almost parallel to the {2-11} plane of the zircon (Fig. DR1).

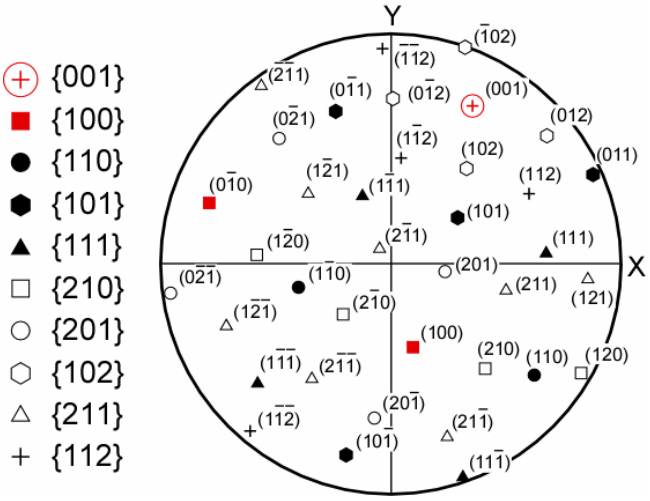

Fig DR1. Lower hemisphere equal area stereographic projection of zircon crystallographic poles at reference point "+" of Fig. 2a. X and Y coordinates correspond to horizontal and vertical borders of Fig. 2a (refer to Fig DR2 for these directions).

Panchromatic cathodoluminescence (PCL) imaging was undertaken at Curtin University, Australia on a Phillips XL30 SEM with an attached KE Developments CL system operating at 12kV and working distance of 15mm. PCL images were collected in the 330-600nm spectral range. Wavelength CL (λCL) data were collected at the Advanced Analytical Centre, James Cook University, Australia, using a Jeol JXA8200 mounted with combined WD/ED electron probe microanalyser (EPMA) with integrated x-ray cathodoluminescence spectrometry system (XCLent) developed by CSIRO Minerals. Operating conditions were 20kV accelerating voltage and 100nA probe current. A 200 x 250µm area was mapped with a grid spacing of 0.5µm using spot size at minimum diameter and 50ms dwell time per point. A standard grating was used with 300 lines/mm and a blaze width of 500nm. λCL data was managed through XCLent operating software, which allowed three different bands of a specific spectral range to be displayed over three color channels.

Zircon U-Th-Pb data were collected using the Sensitive High Resolution Ion MicroProbe (SHRIMP II) housed at the John de Laeter Centre of Mass Spectrometry, Curtin University, Perth, Australia. The sensitivity for Pb isotopes in zircon, with a primary beam current of 2.5-3.0 nA and mass resolution of ~5000, was ~18 cps/ppm/nA. The total Pb signal was dominated by common Pb, leading to large uncertainty in the reduced radiogenic isotope ratios (Table DR1). The quoted $^{206}Pb/^{238}U$ ratio is also corrected for instrumental inter-element discrimination, based on the observed covariation between Pb^+/U^+ and UO^+/U^+ (Hinthorne et al., 1979; Compston et al., 1984) determined from interspersed analyses of the Perth standard zircon CZ3, which is a single zircon megacryst from Sri Lanka with an age of 564 Ma and a $^{206}Pb/^{238}U$ ratio of 0.0914 (Nelson, 1997).

REE data were also collected using SHRIMP II. Analyses were done using SHRIMP under standard operating conditions of mass resolution 5000, at which REE+ and REEO+ peaks are resolvable. Representative species of each element were analyzed (La, Ce, Pr, Nd, Sm, Eu, Gd, Tb, Dy, Ho, Er, Tm, Yb and Lu), isobars subtracted using a REE Excel program (created by Nicholas Padfield, Curtin University) and counts normalized to ppm by ratioing to data for zircon REE standard SL1, whose average ppm abundances have been determined by isotope dilution (analyst Roland Maas – see Table DR2). Problems with peak centering and large oxide interferences on the small LREE peaks in both the standard and the unknown Indian Ocean Zircon compromised the quality of the LREE data. Data for elements La-Sm are therefore not reported.

Geochemical and Isotopic Data

SHRIMP II U-Pb analyses are presented in Table DR1, with analysis locations shown in Fig. DR2. REE data collected by SHRIMP II are shown in Tables DR2 & DR3. Chondrite normalized REE data, calculated using the Chondrite values of McDonough and Sun (1995) are shown in Fig. DR3.

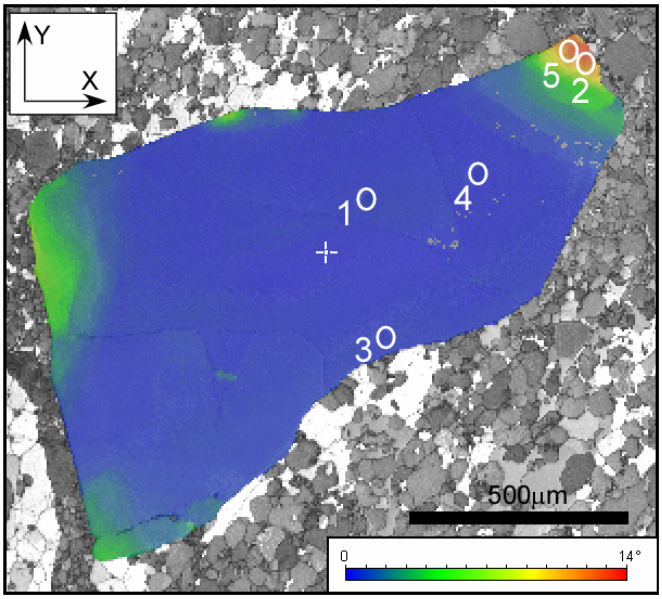

Figure DR2. Location of U-Pb SHRIMP Data shown on EBSD map of zircon (Fig.2a). Numbers correspond to Analysis No. in Table DR1.

TABLE DR1: U-PB SHRIMP AGES FROM INDIAN OCEAN ZIRCON

Analysis No.*	U ppm	Th ppm	Th/U	Pb ppm	%com ^{206}Pb	$^{206}Pb/^{238}U$	± (1σ)	$^{206}Pb/^{238}U$ age (Ma)	± (1σ)
1	3	1	0.34	3	97.2	0.0085	0.0187	55	119
2	6	4	0.67	2	99.9	0.0001	0.0036	1	23
3	5	3	0.54	3	97.4	0.0042	0.0069	27	44
4	4	2	0.42	2	99.0	0.0015	0.0083	10	53
5	6	4	0.68	1	99.0	0.0003	0.0024	2	15
For location see Figure DR2									

TABLE DR2. REE SHRIMP DATA FROM INDIAN OCEAN ZIRCON

Analysis[1,2]	Eu	Gd	Tb	Dy	Ho	Er	Tm	Yb	Lu
1	0.320	7.367	2.910	35.131	14.915	74.852	16.397	168.540	41.215
2	0.304	6.893	2.737	32.839	13.789	70.672	14.946	157.130	39.680
3	0.344	7.387	2.902	35.380	14.582	72.704	15.930	165.735	40.230
4	0.345	7.997	3.092	36.883	15.524	78.073	16.440	171.570	43.002
5	0.358	8.093	3.154	37.627	15.573	77.860	16.656	170.740	42.246
6	0.398	8.543	3.324	37.155	16.147	79.960	17.281	177.262	43.346
7	0.441	9.282	3.444	41.238	16.459	81.522	17.467	180.600	43.804
Norm.[2]	0.323	7.220	2.838	34.929	14.532	74.093	15.815	167.551	41.146
Standard SL1[2,3]	0.201	21.635	6.716*	72.250	29.27*	155.350	35.89*	404.000	100.300

[1] Refer to Fig. 2a of published article for location map
[2] measured as ppm * Interpolated
[3] Refer to Maas et al (1992)

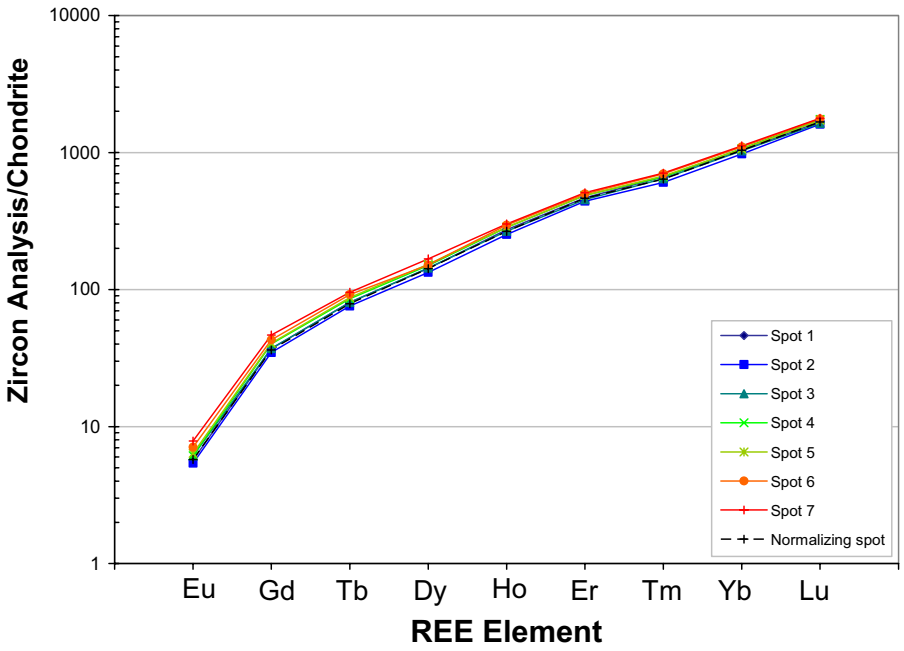

Figure DR3: Chondrite normalized REE data from spots 1-7 and "Normalizing spot" shown in Fig. 2a. Chondrite data used for the normalization was taken from McDonough and Sun (1995). The log scale makes variations between different analyses difficult to resolve, hence the normalization to undeformed zircon in Fig. 3b.

TABLE DR3. NORMALIZED REE SHRIMP DATA FROM INDIAN OCEAN ZIRCON

Analysis*	Eu	Gd	Tb	Dy	Ho	Er	Tm	Yb	Lu
1†	0.99	1.02	1.03	1.01	1.03	1.01	1.04	1.01	1.00
2†	0.94	0.95	0.96	0.94	0.95	0.95	0.95	0.94	0.96
3†	1.06	1.02	1.02	1.01	1.00	0.98	1.01	0.99	0.98
4†	1.07	1.11	1.09	1.06	1.07	1.05	1.04	1.02	1.05
5†	1.11	1.12	1.11	1.08	1.07	1.05	1.05	1.02	1.03
6†	1.23	1.18	1.17	1.06	1.11	1.08	1.09	1.06	1.05
7†	1.37	1.29	1.21	1.18	1.13	1.10	1.10	1.08	1.06
Norm.#	0.32	7.22	2.84	34.93	14.53	74.09	15.82	167.55	41.15

* Refer to Fig. 2a of published article for location map

† Measured as ratio with undeformed zircon from "normalizing analysis" shown in Fig. 2a of published article

measured as ppm

References

Bach, W., Humphris, S.E., Erzinger, J., Dick, H.J.B., Alt, J.C., and Niu, Y., 2001, The geochemical consequences of late-stage low-grade alteration of lower ocean crust

at the SW Indian Ridge: Results from ODP Hole 735B (Leg 176): Geochimica et Cosmochimica Acta, v. 65, p. 3267-3287.

Compston, W., Williams, I.S., and Meyer, C., 1984, U-Pb geochronology of zircons from lunar breccia 73217 using a sensitive high mass-resolution ion microprobe: Journal of Geophysical Research, v. 89, p. B525-B534.

Dick, H.J.B., Bach, W., Bideau, D., Gee, J.S., Haggas, S., Hertogen, J.G.H., Hirth, G., Holm, P.M., Ildefonse, B., Iturrino, G.J., John, B.E., Kelley, D.S., Kikawa, E., Kingdon, A., LeRoux, P.J., Maeda, J., Meyer, P.S., Miller, D.J., Naslund, H.R., Niu, Y.L., Robinson, P.T., Snow, J., Stephen, R.A., Trimby, P.W., Worm, H.U., Yoshinobu, A., Natland, J.H., and Alt, J.C., 2000, A long in situ section of the lower ocean crust: Results of ODP Leg 176 drilling at the Southwest Indian Ridge: Earth and Planetary Science Letters, v. 179, p. 31-51.

Hinthorne, J.R., Anderson, C.A., Conrad, R.L., and Lovering, J.F., 1979, Single-grain $^{207}Pb/^{206}Pb$ and U/Pb age determinations with a 10 μm spatial resolution using the ion microprobe mass analyser (IMMA): Chemical Geology, v. 25, p. 271-303.

Maas, R., Kinny, P.D., Williams, I.S., Froude, D.O. and Compston, 1992, The Earth's oldest known crust: A geochronological and geochemical study of 3900-4200 Ma old detrital zircons from Mt. Narryer and Jack Hills, Western Australia: Geochimica et Cosmochinica Acta, v. 56, 1281-1300.

McDonough, W.F. and Sun, S., -S., 1995, The composition of the Earth: Chemical Geology, v. 120, 223-253.

Natland, J.H., and Dick, H.J.B., 2001, Formation of the lower ocean crust and the crystallization of gabbroic cumulates at a very slowly spreading ridge: Journal of Volcanology and Geothermal Research, v. 110, p. 191-233.

Nelson, D.R., 1997, Compilation of SHRIMP U-Pb zircon geochronology data, 1996, Geological Survey of Western Australia, Perth, Australia.

Trimby, P., 2005, The role of Fe-Ti oxides in the localisation of deformation in ocean gabbro, *in* Kunze, K., ed., 15th Conference on Deformation mechanisms, Rheology and Tecotnics: Zurich, Switzerland, p. 217.